

A Novel AE Based Algorithm for PD Localization in Power Transformers

Sina Mehdizadeh*, Mohammadreza Yazdchi** and Mehdi Niroomand†

Abstract – In this paper, a novel algorithm for PD localization in power transformers based on wavelet de-noising technique and energy criterion is proposed. Partial discharge is one of the main failures in power transformers. The localization of which could be very useful for maintenance systems. Acoustic signals due to a PD event are transient, irregular and non-repetitive. So wavelet transform is an efficient tool for this signal processing problem that gives a time-frequency demonstration. First, different wavelet based de-noising methods are analyzed. Then, a reasonable structure for threshold value determining and applying manner on signals is presented. Evaluated errors are good evidences for choices. Next, applying the elimination low energy frequency bands is discussed and developed as a de-noising method. Time differences between signals are used for PD localization. Different ways in time arrival detection are introduced and a novel approach in energy criterion method is presented. At the end, the quality of algorithm is verified through the different assays in lab.

Keywords: Partial Discharge (PD), Power Transformer, Acoustic Emission, Localization.

1. Introduction

Transformers are important and expensive parts in power systems, and their interrupts are not affordable. So monitoring them to prevent wasting time and financial losses due to their shut down and maintenance is inevitable. During the life time of a power device, because of mechanical, thermal or electrical pressure, insulation may be damaged that may cause catastrophic destruction [1-6].

Partial Discharge is one of the main failures in power transformers. PD starts its activity impalpable but can cause fundamental damages. PD occurs when electrical field change leads to produce the local stream. This stream indicates itself as an electrical pulse that is measureable in transformer output [7].

Because PDs cause insulation breakdown and mechanism of further insulation damage, detection and localization are done to estimate condition and identify problems with insulation of power transformers. In recent years, several methods for detection and localization of PD in power transformers have been developed, which can be classified into four categories of Electrical, Chemical, Acoustic and Optical methods depending on detection quality [8-13].

Acoustic method has high immunity against electromagnetic interferences. Because of better signal to noise

ratio, this immunity makes the acoustic method ideal [13]. Another advantage of acoustic method is PD localizing using information obtained from ultrasonic sensors around the transformer tank [14]. There are two acoustic methods including acoustic systems with an electrical trigger and the all-acoustic systems. All acoustic systems, because of sensors positions, can be divided into internal and external systems. The external system has another preference which is portable and invasive and can be implemented online in transformers [15]. This study focuses on external all acoustic PD measurement systems in oil-immersed power transformers.

In AE Based localization, de-noising plays an important role. Noise is a serious problem through the acoustic method. In a factory, there is a lot of noise, but many of this is not in frequency range of acoustic PD. Detecting the starting point of acoustic signal is very important for localization; therefore, every signal except PD acoustic wave is interpreted as a noise even an acoustic PD signal that is captured through the tank wall and not directly. So others have introduced some methods to de-noise AE produced by partial discharge [3, 10, 13] and [17-21]. Also some methods for localization such as peak criterion are proposed in [12, 18, 22] and [25].

The aim of this study is designing an algorithm for de-noising of acoustic signals produced by partial discharge and localizing of it in oil-immersed transformers via external all acoustic measurement to implement practically in future for power transformers.

This paper first investigates wavelet based de-noising methods. Then AE based localization methods is considered. Finally an effective algorithm for de-noising

† Corresponding Author: Dept. of Electrical and Electronic Engineering, University of Isfahan, Iran. (Mehdi_niroomand@eng.ui.ac.ir)

* Dept. of Electrical and Electronic Engineering, Islamic Azad University, Bushehr branch, Iran. (sina.mehdizadeh@yahoo.com)

** Dept. of Biomedical Engineering, University of Isfahan, Iran. (yazdchi@eng.ui.ac.ir)

Received: December 8, 2012; Accepted: June 17, 2013

and localizing is presented.

2. Wavelet Based De-noising

Noise is the fundamental limit in the partial discharge test. Methods are proposed by the existing standard [16] based on the time and frequency field that each is effective only on certain types of noise. Employing this method, Require knowledge of the presence of noise and be under consideration online PD is very difficult [17].

The partial Discharge pulses are transient, irregular and non-repetitive. Analyzing events in infinite range is the Fourier fundamental problem. A signal breaks to frequency harmonics which oscillate unlimited with fixed period and don't have local features in time domain. As a result, information are carried by discharges pulse such as starting time aren't clear [17].

2.1. Discrete Wavelet Transform (DWT) properties

Wavelet Transform (WT) is a mathematical tool that was designed to analyze the transient, irregular and non-iterative signals in a phase – space (time - scale or time - frequency). Due to the capability of wavelet Transform to remove noise from signals for example in the earthquake science and multimedia technology, this is an essential tool to extract partial discharge signals in noisy environments. Because the PD signals have transient, irregular and non-iterative nature too.

2.1.1. DWT filter pair structure

The DWT results is a series of coefficients including the approximation and several details that are presented by $Ca_N, Cd_N, Ca_{N-1}, \dots, Cd_2, Cd_1$ where N is the final decomposing level. Fig. 1 illustrates this process.

When a noisy signal is decomposed, the signal and noise in various levels of decomposition can be observed that present the possibility of separation. Using a threshold for each level, a de-noised signal is reconstructed.

2.1.2. Frequency bands

As described, using DWT is equivalent to filtering a

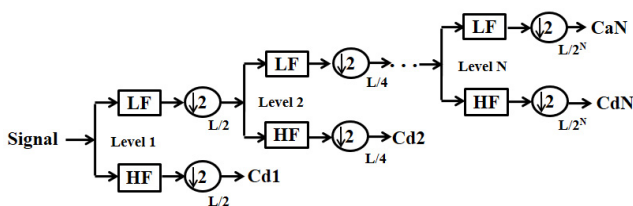


Fig. 1. DWT logarithm tree including filtering and down-sampling

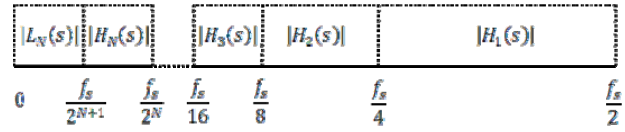


Fig. 2. Filters frequency bands in various decomposition levels

signal with Quadrature Mirror Filters (QMF) [8]. Fig. 2 illustrates the ideal wavelet filters frequency bands.

2.2. DWT de-noising

DWT de-noising method has three steps including [18]:

1. Desired signal decomposing and calculation of wavelet coefficients.
2. Inserting the threshold for the coefficients. For each step, a threshold is chosen and applied on the coefficients. Hence, de-noising includes selecting the signal coefficients and elimination of the noise coefficients.
3. Signal reconstruction. Signal reconstruction is based on modified approximation and details coefficients.

2.2.1. Threshold determining

Threshold selection plays an important role in the process of noise removal. Based on the noise variance, four common threshold estimating methods are presented [19]:

• General Threshold

$$Thr = \sqrt{2 \log n} \quad (1)$$

Where n is the length of noisy signal.

• Minimaxi Threshold

$$Thr = \begin{cases} \sigma(0.3936 + 0.1829 \log_2 n), & n \geq 32 \\ 0, & n < 32 \end{cases} \quad (2)$$

Where n is the length and σ is the deviation of noisy signal.

• Heuristic Stein Unbiased Risk (HSUR) Threshold [20].

$$Thr = \sqrt{2 \log_e (n \log_2 n)} \quad (3)$$

• Level-dependent Threshold

$$\lambda_j = \frac{m_j}{0.6745} \sqrt{2 \log_2 n_j} \quad (4)$$

Where λ_j is the threshold value at level j , m_j is the mean value at level j and n is the length of the signal.

Level-dependent threshold method is widely used in recent papers [21].

2.2.2. Applied manner determining for threshold

After that threshold value was determined, threshold function needed to be selected. Hard thresholding keeps wavelet coefficients that are higher than threshold and removes the rest. Soft thresholding makes zero the wavelet coefficients that are below the threshold, keeping larger coefficients and then shrinking towards zero.

PD energy and its properties can be saved in hard threshold functions, but through this function a rough signal is obtained. Through soft threshold functions, a smooth signal is achieved, but the energy of PD is lost [19]. Threshold function Mark softens PD filter can provide the signal, but the energy is lost.

2.2.3. Evaluation of noise rejection effect

Mean square error (MSE) and measure error (ME) are used to indicate the effect of noise removal, and are defined below [19]:

$$MSE = \frac{1}{n} \sum_{i=1}^n [f(i) - r(i)]^2 \tag{5}$$

Where f is the original pulse signal, r is the de-noised PD signal and n is the length of signal.

$$MSE = \frac{A_f - A_r}{A_f} \times 100 \tag{6}$$

Where A_f is the original signal domain and A_r is the de-noised PD signal domain.

3. AE based PD localization

A graphical view of a transformer tank with 4connected sensors, PD inside the transformer and the obtained distances D_i are shown in Fig. 3. These variables are used to form geometric relations. PD event is modeled as a point

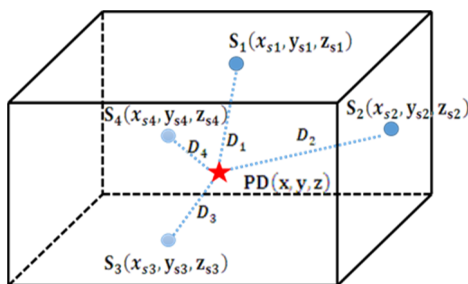


Fig. 3. Acoustic sensors Cartesian coordinate on tank wall of transformer

which emits acoustic wave in a homogeneous environment (here in Oil). Corresponded nonlinear equations are characterized by spherical functions, which focuses on the PD source. A corner of tank is chose as center of coordinate.

For making a relation between the introduced variables in Fig. 3 and eventually establishing nonlinear equations for localization, there are several methods such as time-difference method, absolute-time method and pseudo-time method. Because of using all acoustic systems, in this paper, time-difference method is used to form the equations.

3.1. Time-difference approach

Time- difference method is appropriate for all acoustic measuring in which an acoustic trigger is used for other channels. In fact, according to Fig. 4, in addition to the PD location, the exact time of PD happening (T) is unknown. Time arrival differences of signals in different sensors toward first sensor which receives signal sooner τ_{ii} , are available.

Time- difference method is appropriate for all acoustic measuring in which an acoustic trigger is used for other channels. In fact, according to Fig. 4, in addition to the PD location, the exact time of PD happening (T) is unknown. Time arrival differences of signals in different sensors toward first sensor which receives signal sooner τ_{ii} , are available.

$$(x - x_{s1})^2 + (y - y_{s1})^2 + (z - z_{s1})^2 = (v_s T)^2 \tag{7}$$

$$(x - x_{s2})^2 + (y - y_{s2})^2 + (z - z_{s2})^2 = (v_s (T + \tau_{12}))^2 \tag{8}$$

$$(x - x_{s3})^2 + (y - y_{s3})^2 + (z - z_{s3})^2 = (v_s (T + \tau_{13}))^2 \tag{9}$$

$$(x - x_{s4})^2 + (y - y_{s4})^2 + (z - z_{s4})^2 = (v_s (T + \tau_{14}))^2 \tag{10}$$

In these equations, (x, y, z) is PD location coordinate, (x_{si}, y_{si}, z_{si}) is the sensor i coordinate, τ_{ii} is the time arrival difference of acoustic signal in sensor i toward first sensor, T is the time arrival of acoustic signal is reached by first sensor and v_s is the velocity of sound in oil.

As is clear from equations above, solving the equations requires achieving the time arrival differences of acoustic signals due to partial discharge that is received by sensors.

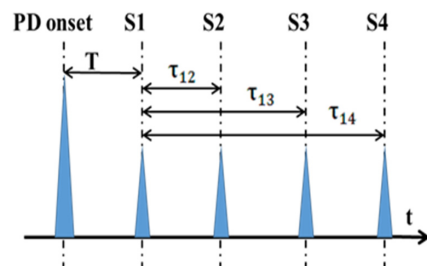


Fig. 4. Time-differences between four sensors

3.2. Time arrival determination

The First step into localization of partial discharge is determination of time arrival of signals for time differences calculation. Several different criteria for time arrival determination are surveyed.

3.2.1. Peak criterion

One of the time arrival determination methods is the peak criterion. A threshold is applied on signal and time of first crossing through the threshold is determined. This time can be considered as PD pulse arrival time. In this method, the value of threshold according to Eq. (11) is 20 percent of signal's max and liking two parallel horizontal lines is proposed [18]. The schematic is shown in Fig. 5.

$$Thr = 0.2 \times Max \dots if \dots Max > 4 \times 10^{-5} \quad (11)$$

Where MAX is the signal's extremum. This value is obtained after several experiments [18].

One of the time arrival determination methods is the peak criterion. A threshold is applied on signal and time of first crossing through the threshold is determined. This time can be considered as PD pulse arrival time. In

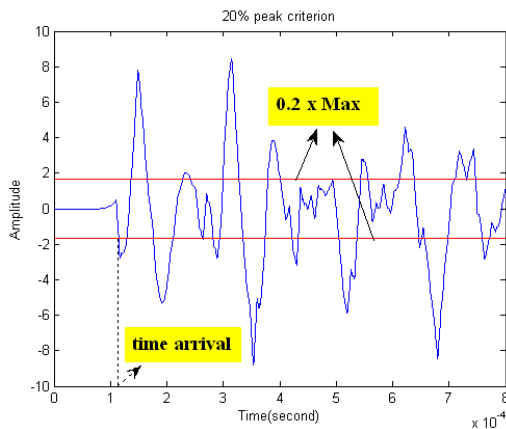


Fig. 5. Determination of signal's time arrival graphically

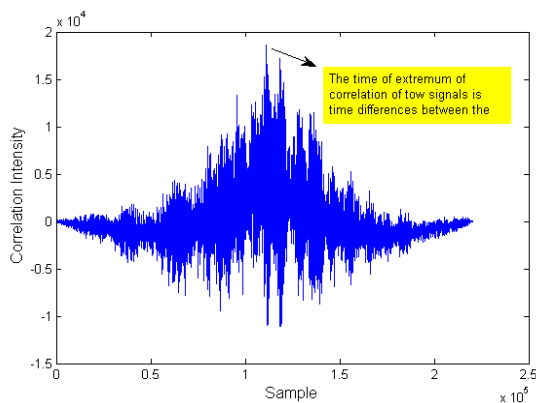


Fig. 6. Correlation criterion for time arrival determination

this method, the value of threshold according to Eq. (11) is 20 percent of signal's max and linking two parallel horizontal lines is proposed [18]. The schematic is shown in Fig. 5.

3.2.2. Correlation criterion

Alternative method to find the time difference between two signals, is the correlation between them. When two signals received by two sensors are similar except for the delay time and intensity, the time delay can be determined via the time of the extremum of correlation diagram. This process is illustrated in Fig. 6. If two signals are the same, the peak occurs at zero.

3.2.3. Energy criterion

One of the other criteria for determining the arrival time, is energy criterion. This criterion is based on this fact that most of the time the acoustic signals are known by change of their energy component rather than their frequency components [6]. Energy curve S_i is a cumulative sum of signal samples values while partial energy at each points, according to Eq. (12), is subtracting energy till that point from a trend.

$$S'_i = S_i - i\delta = \sum_{k=0}^i (x_k^2 - i\delta) \quad (12)$$

Where i is the loop variable which exchanges for all signal samples, δ is a negative trend that is related to the total signal energy S_N and length of signal N which is defined via Eq. (7).

$$\delta = S_N / (\alpha N) \quad (13)$$

Fig.7 illustrates the partial energy curve before reaching the energetic part of signal has a negative slope. But after that it rises up. This turning point introduces a min. The time of this min is assumed corresponding to the time of signal onset [22].

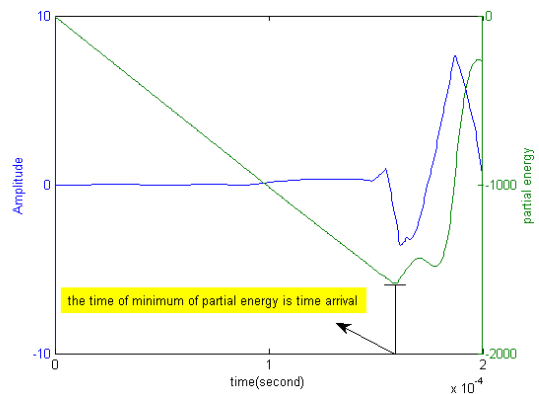


Fig. 7. Occurrence time of the partial energy minimum as signal time arrival

4. Experimental Results

First, the qualifications and conditions of PD simulation in lab are explained. Next described techniques in the previous section is implemented. Finally, the results are presented.

4.1. Case study of PD

PDs are produced in a $0.3 \times 0.3 \times 0.6 \text{ m}^3$ tank that is filled with oil and the acoustic signals are received by four ultrasonic sensors on the outer walls of the tank. The four sensors in terms of distance from the PD source are located so that signals are received via two sensors directly and via two sensors indirectly and through the tank wall. Because of the long distance from the PD source and this fact that velocity of sound in oil is not as much as in metal, two

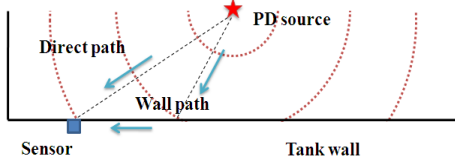


Fig. 8. Emission in various directions

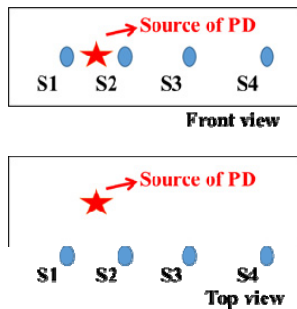


Fig. 9. A view of sensors arrangement on thank wall

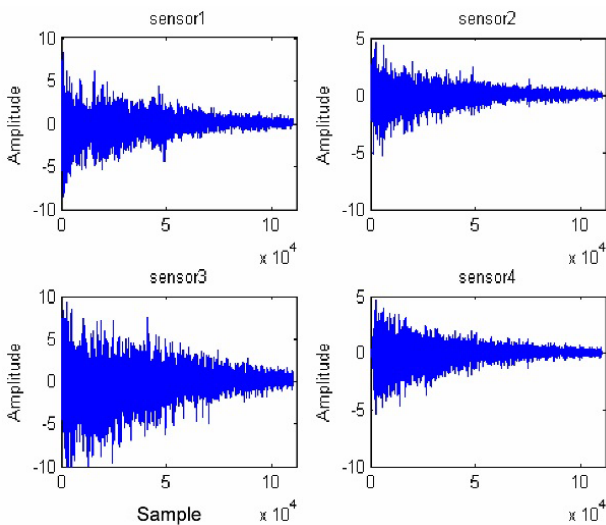


Fig. 10. Received signals to four sensors on thank wall

sensors receive signals through the wall first and then receive direct signal. The schematic is shown in Figs. 8 and 9. These signals are produced three times with changing the location of sensors and PD source.

Received signals are amplified 40dB, sampling frequency is 2.5 MHz and in each sampling, 150,000 samples have been captured. In Fig. 10, received signals by the four sensors are given in the first test.

4.2. De-noising results

There is a common equation to determine the numbers of levels in the wavelet decomposition:

$$N = \text{fix} \left[\log_2 \left(\frac{n}{n_w} - 1 \right) \right] \tag{13}$$

Where n is the length of original signal and n_w is the length of mother wavelet function. According to the 150,000 samples, via Eq. (14), 14 levels is achieved that according to the Table 1and also PD frequency bands, 14 levels is unreasonable and 9 levels is adequate. Finally the truth of this selection is proved.

Signal processing is done in MATLAB software. In addition for signal decomposition, db3 is used as a mother wavelet function that following frequency bands is shown in Table 1.

After selecting the mother wavelet and number of decomposition levels, a threshold criterion and applying style are chosen. Threshold selection plays an important role in de-noising process. Different results are given via soft and hard threshold.

Mixture threshold, is a combination of the general threshold and HSUR. Since the aim is selecting a wavelet de-noising method and studying the signal's energy, hard threshold is selected because signal's energy is preserved although a rough signal is presented. In this step also the MEs and MSEs are observed.

Several models such as brigé-massart model [24], the model based on Gaussian white noise, the model based on non-Gaussian white noise, automatic model and level-dependent model for threshold selecting are studied so that the value of threshold is obtained from above threshold estimating methods.

First 1000samples of signal which is received by means of sensor 3 are demonstrated by Fig. 11. The primary fluctuations of signal are surface signal that is received from the tank wall. De-noised signal is achieved via the

Table 1. Details frequency bands

D1	1250-625 kHz	D6	39-19.5 kHz
D2	625-312.5 kHz	D7	19.5-9.7 kHz
D3	312.5-156 kHz	D8	9.7-4.8 kHz
D4	156-78.1 kHz	D9	4.8-2.4 kHz
D5	78.1-39 kHz	A9	0-2.4 kHz

model based on Gaussian white noise and hard threshold is shown in Fig. 12. The original signal is blue and de-noised signal is red. Appropriate ME is shown in Fig. 13.

With comparison between Figs. 11 and 14, it's obvious that this model not only destroys the primary parts of signal, but the fluctuations related to surface wave is also

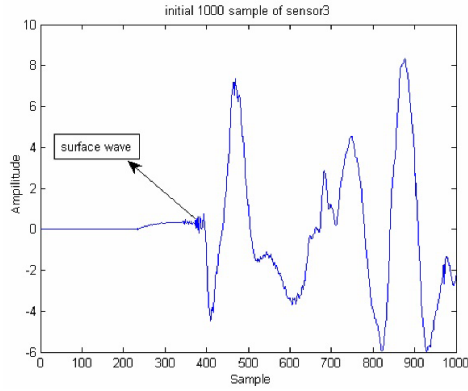


Fig. 11. First 1000 samples of signal is received via sensor 3

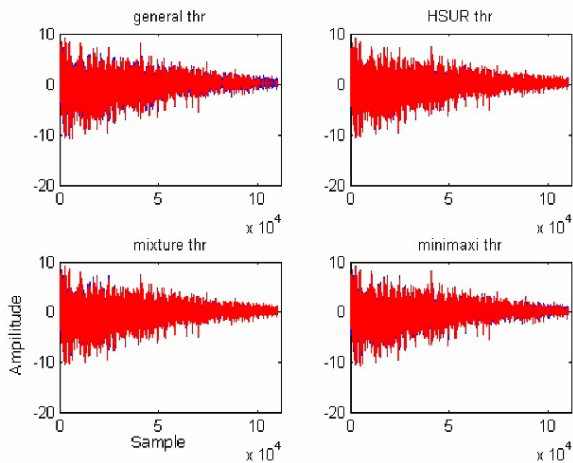


Fig. 12. De-noised signal with a model based on Gaussian white noise

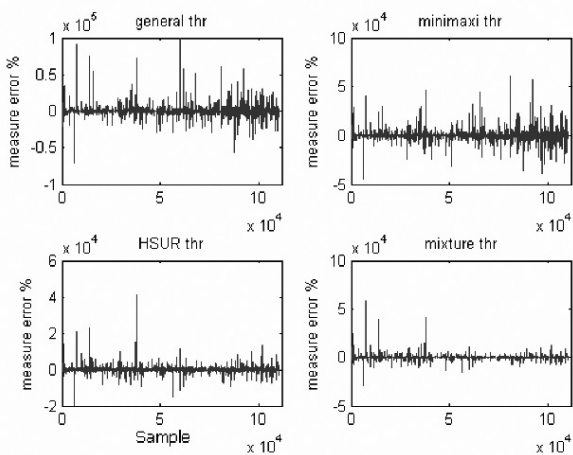


Fig. 13. Measure error in the model based on Gaussian white noise

considered as noise and is omitted. Also general and mixture threshold present the best performance.

According to Figs. 11-14, Tables 2-5 and the analyses, it seems the combination of the model based on Gaussian white noise and the calculated value via mixture threshold approach through the 9 level decomposition is the best choice. Dependence of wavelet based de-noising method to decomposition levels is another finding. So in order to prevent the excessive details, it is better to choose Nyquis

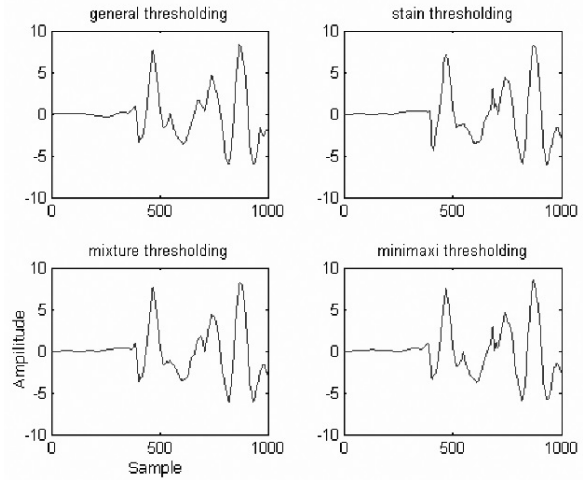


Fig. 14. First 1000 primary de-noised signal via in the model based on Gaussian white noise

Table 2. Mean square error of direct soft and hard thr

Direct Thresholding	Soft	Hard
General	3.4773	2.6617
Minimaxi Thr	2.7316	1.7692
HSUR Thr	0.4018	0.0676
Mixture	0.4018	0.0676

Table 3. Mean square error of level-dependent hard and soft thresholding via mean and median

Level-dependent Method	Soft	Hard
Median	0.0459	0.0022
Mean	0.2581	0.1184

Table 4. Mean square error of model based on Gaussian white noise thresholding and without it

Model based on	Gaussian white noise	Non Gaussian white noise
General Thr	0.2312	3.3880
Minimaxi Thr	0.1309	2.6327
HSUR Thr	0.0213	0.3367
Mixture	0.0394	1.3479

Table 5. Mean square error of brigé-massart and automatic thresholding in 7, 8 and 9 levels

Decomposition Level	7 levels	8 levels	9 levels
brigé-massart	1.2792	0.8718	0.3919
Automatic thresholding	-	-	0.06

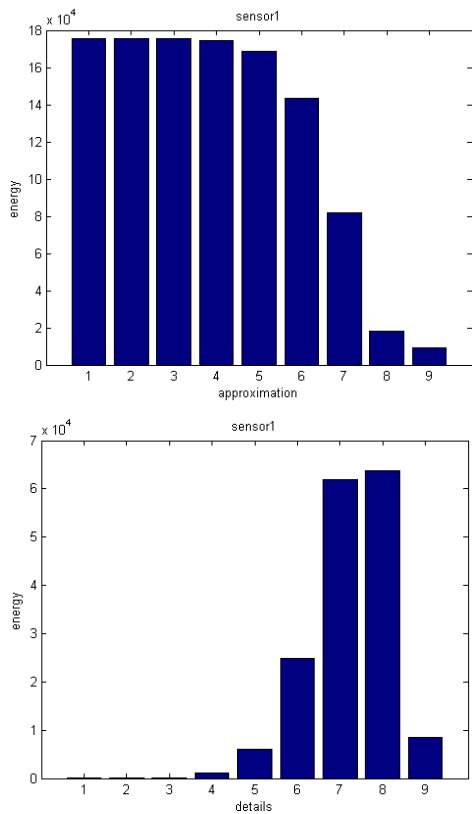


Fig. 15. Details and approximation energy of signal is received via sensor 1

trate for sampling rate precisely.

4.2.1. Details energy distribution

In this section, the details energy is studied.

$$EA_k = \sum_{i=1}^{N_k} (Ca_i)^2 \tag{14}$$

$$ED_k = \sum_{i=1}^{N_k} (Cd_i)^2 \tag{15}$$

Where EA_k is the total energy of approximation coefficients in k levels, EA_k is the total energy of details coefficients in k levels and N_k is the length of signal in that level. In Fig. 15, details and approximation energy of signal is received via sensor 1 is demonstrated.

Reconstructed signal is obtained by means of Eq. (16):

$$\begin{aligned} &Reconstructed..Signal \\ &= IDWT(Ca_0 + Cd_0 + Cd_8 + \dots + Cd_1) \end{aligned} \tag{16}$$

Where Ca is approximation coefficient and Cd is detail coefficient.

According to Fig. 15, negligible energy is put in d1, d2, d3 and a9 which can be ignored as the unwanted signals via Eq. (16). Also the most part of energy is distributed in details 7 and 8 corresponding to 5-20 kHz frequency

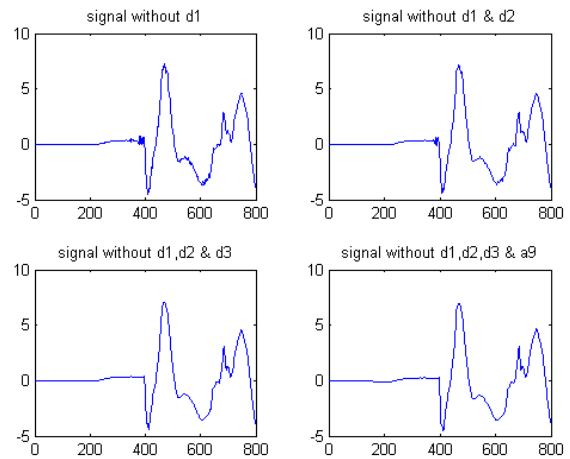


Fig. 16. First 800 primary samples of signal is received through d1, d2, d3 and a9.

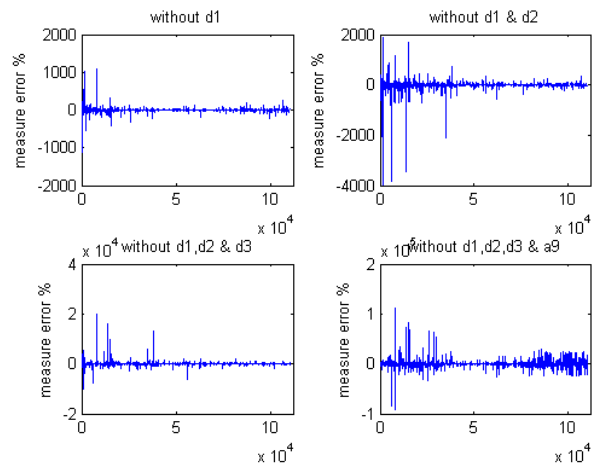


Fig. 17. Measure error of d1, d2, d3 and a9 omission

ranges. Useful information is provided via this fact. Also this energy distribution through the change of sampling rate or discharge type is varied.

According to Figs. 15-17 and Table 6 as expected, omission of d1, d2, d3 and a9 operate as an excellent system to de-noise signal and primary fluctuations of signal produced by surface wave is omitted well. Mean square error and amplitude error demonstrate that the omission of a9 is not necessary.

Finally in de-nosing, mother wavelet db3, 9 level of decomposition, hard thresholding through the model based on Gaussian white noise using value that is obtained from mixture threshold method and omitting of d1, d2 and d3 are the best selection.

4.3. Localization results

In this section, the described time arrival detection methods are compared. A criterion is needed to compare, so the time of first negative peak of acoustic signal is chosen. This process is illustrated in Fig. 18.

In Table 7, this time is determined for signals which are received via four sensors in three assays.

In Tables 8-10, times arrival via correlation criterion, peak criterion and energy criterion are calculated respectively.

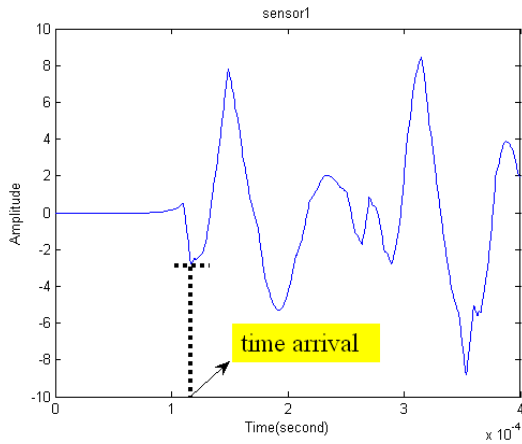


Fig. 18. The time of first negative peak as time arrival graphically

Table 6. Mean square error of d1, d2, d3 and a9

	Without d1	Without d1 & d2	Without d1, d2 & d3	Without d1, d2, d3 & a9
Mean Square Error	5.9679×10^{-5}	3.406×10^{-4}	0.0028	0.2052

Table 7. Time arrival of signals which are received via sensors in three assays

Assay	Sensor 1	Sensor 2	Sensor 3	Sensor 4
1	116.8 μ s	122.8 μ s	161.6 μ s	244.4 μ s
2	122.8 μ s	122.8 μ s	167.6 μ s	244.4 μ s
3	122.8 μ s	122.8 μ s	161.6 μ s	161.6 μ s

Table 8. Time differences arrival of signals via correlation criterion in three assays

Assay	S_1-S_2	S_1-S_3	S_1-S_4
1	-240 μ s	898.4 μ s	340 μ s
2	-241.2 μ s	150.8 μ s	343.2 μ s
3	-240 μ s	157.2 μ s	157.2 μ s

Table 9. Time arrival of signals via peak criterion in three assays

Assay	Sensor 1	Sensor 2	Sensor 3	Sensor 4
1	115.6 μ s	120 μ s	160 μ s	257.6 μ s
2	117.6 μ s	120.4 μ s	161.2 μ s	462 μ s
3	115.6 μ s	119.6 μ s	159.6 μ s	159.6 μ s

Table 10. Time arrival of signals via energy criterion in three assays

Assay	Sensor 1	Sensor 2	Sensor 3	Sensor 4
1	114 μ s	118.4 μ s	159.6 μ s	540 μ s
2	115.2 μ s	118.8 μ s	160.4 μ s	459.2 μ s
3	113.6 μ s	118 μ s	158.8 μ s	158.8 μ s

With comparison between Tables 7 and 8, it's obvious that time differences are obtained from correlation criterion is different from absolute times completely because the signals are not same exactly.

Also comparison between Tables 7 and 9 shows that peak criterion has a better performance rather than correlation, although an irrelevant time is obtained.

According to Tables 7 and 10 and Fig. 19, in some signals which have low energy primary part, usage of energy criterion is not reasonable, for example signals which are received via sensor 4 in this experiment. It is because the low energy part can't change the slope of partial energy curve and make a minimum timely. Therefore a new criterion is introduced which is the time of local minimum in partial energy curve as time arrival (Fig. 19 and Eq. (17)).

$$S_n'' = S_{n+1}' - S_n' \quad (17)$$

Where S_n' is the partial energy in sample n and S_n'' is the differential of partial energy in that sample.

The reached times arrival through the differential partial energy criterion are given in Table 11. With comparison between Tables 7 and 8-11, it's realized that the differential partial energy criterion is the best choice.

After determining the time arrival of signals, the localization equations are formed, and Time difference approach is chosen. In this approach the time arrival of signal is reached by first sensor T is not available but time differences between signals τ_{i_i} are valid. Also the sound velocity in oil $V_s = 1413$ m/s is assumed [15]. Results are shown in Table 12.

According to Table 12, the greatest difference between the coordinates calculated by the algorithm and PD

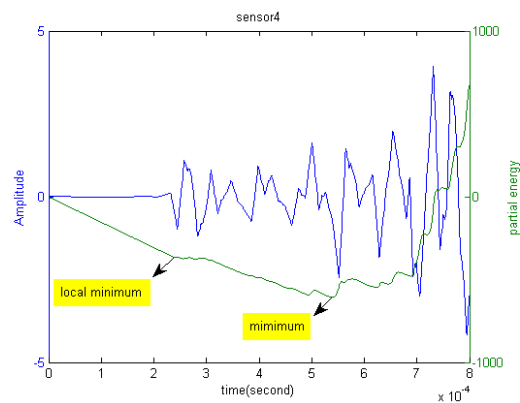


Fig. 19. Partial energy in signals with low energy beginning

Table 11. Time differences arrival of signals via differential energy criterion in three assays

Assay	Sensor 1	Sensor 2	Sensor 3	Sensor 4
1	114 μ s	118.4 μ s	159.6 μ s	242.8 μ s
2	115.2 μ s	118.8 μ s	160.4 μ s	240.8 μ s
3	113.6 μ s	118 μ s	158.8 μ s	158.8 μ s

Table 12. Result of the localization algorithm (all coordinates are in mm)

Assay	1	2	3
Sensor 1 (x,y,z)	(300,0,150)	(300,0,150)	(300,0,120)
Sensor 2 (x,y,z)	(310,300,200)	(300,300,80)	(300,300,120)
Sensor 3 (x,y,z)	(170,72,300)	(355,60,300)	(435,200,300)
Sensor 4 (x,y,z)	(577,250,0)	(500,150,0)	(155,150,0)
PD Source Position (x,y,z)	(300,150,150)	(110,160,150)	(300,150,150)
PD Source Position Calculated by Algorithm	(293,152,142)	(98,150,140)	(332,146,119)

coordinates is only 32 mm. So the error of algorithm is under 35 mm and about 7%. Therefore, the success of localization algorithm is clear.

5. Conclusion

Wavelet transform is a suitable method to de-noise the acoustic signal due to partial discharge in power transformers. A novel algorithm based on wavelet for denoising and localizing acoustic signals is presented which according to the results, is successful. In this algorithm, there is a nine-level decomposition, and the threshold value is determined through the mixture threshold method and applied via the model based on Gaussian white noise. Omission of low energy frequency bands as unwanted signal is presented and developed. The number of decomposition levels can be verified through the frequency bands energy diagram. In addition, dependence of wavelet based de-noising on the number of decomposition levels is demonstrated.

The PD source location is determined via this algorithm with very little error. So, it is clear that using of differential of partial energy criterion is the best method. In this paper, the algorithm for three assays with relocation of PD source and sensors is examined and the results are acceptable.

Acknowledgements

This work was supported by Mobarakeh Steel Company. Special thanks to Giscard Veloso and other friends who help us to write this paper.

References

- [1] P. Kundu, N. K. Kishore, and A. K. Sinha, "Classification of Acoustic Emission Based Partial Discharge in Oil Pressboard Insulation System Using Wavelet Analysis," *International Journal of Electrical and Electronics Engineering*, Vol. 1, No. 4, pp. 208-215, 2008.
- [2] T. Boczar and D. Zmarzły, "Application of Wavelet Analysis to Acoustic Emission Pulses Generated by Partial Discharges," *IEEE Trans. Dielectrics and Electrical Insulation* Vol. 11, No. 3, pp. 433-449, Jun. 2004.
- [3] E. Grossman and K. Feser, "Sensitive Online PD-Measurements of Onsite Oil/Paper-Insulated Devices by Means of Optimized Acoustic Emission Techniques (AET)," *IEEE Trans. Power Delivery*, Vol. 20, No. 1, pp. 158-162, Jan. 2005.
- [4] A. Kelen, "Trends in PD diagnostics. When new options proliferate, so do old and new problems," *IEEE Trans. Dielectrics and Electrical Insulation*, Vol. 2, No. 4, pp. 529-534, Aug. 1995.
- [5] J. L. Kirtley, J. C. Lavalley and D. J. McCarthy, "Acoustic monitoring of transformer structures," In *Proc. CIGRE Symposium on "New and Improved Materials for Electro-Technology"*, Vienna, Austria, 1987, pp. 1-5.
- [6] S. Rengarajan, A. Bhoomaiah, K. Krishna and Kishore, "Acoustic PD measurements for transformer insulation-an experimental validation", In *Proc. Eleventh Inter-national Symposium on High Voltage Engineering.*, Singapore, 1999, pp. 1-8.
- [7] E. Mohammadi, M. Niroomand, M. Rezaeiarr', Z. Amini, "Partial Discharge Localization and Classification Using Acoustic Emission Analysis in Power Transformer," In *Proc. INTELEC2009*, pp. 1-6.
- [8] M. Duval, "Dissolved gas analysis: It can save your transformer," *IEEE Electrical Insulation Mag.*, Vol. 5, No. 1, pp. 22-27, Jan./Feb. 1989.
- [9] M. Duval, "A review of faults detectable by gas-in-oil analysis in transformers," *IEEE Electrical Insulation Mag.*, Vol. 18, No. 3, pp. 8-17, May/June 2002.
- [10] G. C. Stone, "Partial discharge. VII. Practical techniques for measuring PD in operating equipment," *IEEE Electrical Insulation Mag.*, Vol. 7, No. 4, pp.9-17, Jul./Aug. 1991.
- [11] L. E. Lundgard, "Partial Discharge — Part XIV: Acoustic Partial Discharge Detection — practical application," *IEEE Electrical Insulation Mag.*, Vol. 8, No. 5, pp. 34-43, Sep./Oct. 1992.
- [12] P. M. Eleftherion, "Partial discharge. XXI. Acoustic emission based PD source location in transformers," *IEEE Electrical Insulation Mag.*, Vol. 11, No. 6, pp. 22-26, Nov./Dec. 1995.
- [13] L. J. Chen, W. M. Lin, T. P. Tsao, and Y. H. Lin, "Study of Partial Discharge Measurement in Power Equipment Using Acoustic Technique and Wavelet Transform," *IEEE Trans. Power Delivery*, Vol. 22, No. 3, pp. 1575-1580, Jul. 2007.
- [14] S. Y. Choi, D. W. Park, I. K. Kim, C. Y. Park and G. S. Kil, "Analysis of Acoustic Signals Generated by Partial Discharges in Insulation Oil," In *Proc. CMD 2008*, pp. 525-528.
- [15] "IEEE Guide for the Detection and Location of

Acoustic Emissions from Partial Discharges in Oil-Immersed Power Transformers and Reactors,” IEEE Std. C57.127™, 2007.

- [16] British Standard Institution, “British Standard Guide for Partial Discharge Measurements,” 2000.
- [17] X. Zhou, C. Zhou and I. J. Kemp, “An Improved Methodology for Application of Wavelet Transform to Partial Discharge Measurement Denoising”, IEEE Trans. Dielectrics and Electrical Insulation Vol. 12, No. 3, pp. 586-594, June 2005
- [18] X. Song, C. Zhou and D. M. Hepburn, “An Algorithm for Identifying the Arrival Time of PD Pulses for PD Source Location,” In Proc. CEIDP 2008, pp. 379-382.
- [19] W. Li, J. Zhao, “wavelet-based de-noising method to online measurement of partial discharge,” In Proc. APPEEC 2009, pp. 1-3.
- [20] X. P. Zhang, M. D. Desai, “Adaptive denoising based on SURE risk,” IEEE Signal Processing Letters, Vol.5, No.10, pp.265-267, Oct. 1998.
- [21] X. Ma, C. Zhou and I. J. Kemp, “Automated Wavelet Selection and Thresholding for PD Detection,” IEEE Electrical Insulation Mag., Vol.18, No.2, pp.37-45, Mar./Apr. 2002.
- [22] S. M. Markalous, S. Tenbohlen and K. Feser, “Detection and Location of Partial Discharges in Power Transformers using Acoustic and Electromagnetic Signals,” IEEE Trans. Dielectrics and Electrical Insulation Vol. 15, No. 6, pp. 1576-1583, Dec. 2008.
- [23] G. F. C. Veloso, L. E. B. da Silva, G. Lambert-Torres, J. O. P. Pinto, “Localization of Partial Discharges in Transformers by the Analysis of the Acoustic Emission,” In Proc. ISIE 2006, pp. 537-541.
- [24] L. Birgé, P. Massart, “From model selection to adaptive estimation,” in D. Pollard (ed), Festschrift for L. Le Cam, New York: Springer, 1997, pp. 55-88.
- [25] G. S. Kil, D. W. Park, I. K. Kim, S. Y. Choi, “Analysis of Partial Discharge in Insulation Oil using Acoustic Signal Detection Method,” WSEAS Trans. Power Systems, Vol. 3, No. 3, pp. 90-94, Mar. 2008.



Mohammadreza Yazdchi Mohammadreza Yazdchi obtained his B.Sc. in Electrical Engineering from the Isfahan University of Technology in 1997. He received his M.Sc. And Ph.D. in Biomedical Engineering from Amirkabir University of Technology 2000 and 2006 respectively. He is currently an

Assistant Professor in the Department of Biomedical Engineering at the University of Isfahan since 2007. His research interests include Biomedical Signal Processing, Medical Image Processing, Biomedical Instrumentation, Biologically Inspired Computing and Bio-Inspired Engineering.



Mehdi Niroomand He was born in Isfahan, Iran, in 1979. He received the B.S., M.S. and Ph.D. degree in electrical engineering from Isfahan University of Technology (IUT), Iran in 2001, 2004 and 2010 respectively. Since 2010, he has been with the Department of Electrical Engineering

at University of Isfahan, where he is presently an Assistant Professor. His research interests include power electronics, uninterruptible power supplies, switching power supplies, control in power electronics and renewable energy.



Sina Mehdizadeh He was born in Masjedsoleiman, Iran, in 1983. He received the B.S. degree in biomedical engineering from University of Isfahan and M.S. degree in electronic engineering from Islamic Azad University, Bushehr branch, Iran in 2007 and 2010 respectively. He is currently electrical

engineer in the AGAHAN Engineering & Management Co. since 2011. His research interests include signal processing, wavelet transform, partial discharge, acoustic analyzing and power electronics.